Nisula, Mikko; Linnera, Jarno; Karttunen, Antti J.; Karppinen, Maarit

Lithium Aryloxide Thin Films with Guest-Induced Structural Transformation by ALD/MLD

Published in:
CHEMISTRY: A EUROPEAN JOURNAL

DOI:
10.1002/chem.201605816

Published: 01/01/2017

Document Version
Publisher's PDF, also known as Version of record

Please cite the original version:
Nisula, M., Linnera, J., Karttunen, A. J., & Karppinen, M. (2017). Lithium Aryloxide Thin Films with Guest-Induced Structural Transformation by ALD/MLD. CHEMISTRY: A EUROPEAN JOURNAL, 2988 – 2992. https://doi.org/10.1002/chem.201605816

Experimental Details

The samples were deposited using an F-120 flow-type hot-wall ALD reactor (ASM Microchemistry Ltd.), from lithium bis(trimethylsilyl)amine (LiHMDS, 97 %, Sigma Aldrich), and hydroquinone (HQ, >99.5 %, Merck KGaA). Both precursors were kept inside the reactor at temperatures of 60 °C for LiHMDS and 95 °C for HQ. The Al_2O_3 capping layer was deposited using trimethylaluminum and H_2O. Nitrogen (99.999%, produced from air by Schmidlin UHPN 3000 nitrogen generator) was used both as purging and carrier gas. The films were deposited on Si(100) for general characterization and on borosilicate for the UV/VIS measurements. The reactor pressure was ~5 mbar. The sample thickness and crystallinity was determined with X-ray reflectivity (XRR) and grazing incidence X-ray diffraction (GIXRD), respectively using a PANanalytical X'Pert Pro diffractometer with a Cu K_α X-ray source. The thickness, density and roughness values were extracted from the XRR data by fitting with the PANanalytical X-ray Reflectivity software taking into account the Al_2O_3 capping layer. The LeBail profile fitting of the GIXRD data was conducted using the FullProf Software Suite[1]. The IR data was collected with a Nicolet Magna 750 FTIR spectrometer in transmission mode on samples deposited on Si in range of 400-4000 cm^{-1} using a resolution of $4cm^{-1}$. The spectrum of bare Si was subtracted from the sample data. The atomic force microscopy (AFM) images were obtained with a Bruker Nanoscope V device operated in tapping mode. The UV/VIS measurements were conducted with a Hitachi U-2000 spectrophotometer in range of 200 - 1100 nm. The absorbance data was deduced from transmittance and reflectance measurements and the optical band gap was estimated from the square of the absorption coefficient plotted against the photon energy.

Computational Details

All density functional calculations, including full structural relaxation of both atomic positions and cell parameters, and vibrational properties at the Γ-point, were performed with the CRYSTAL14 program package.[2-5] We applied the PBE0 hybrid functional method, which incorporates 25% of the Hartree-Fock exchange energy and 75% of the PBE exchange energy.[6,7] A modified all-electron, Gaussian-type basis set based on the molecular Karslruhe triple-ζ-valence + polarization (TZVP) basis set was used in the solid-state calculations (full basis set details are given below).[8] A grid of 4×6×4 *k*-points in the Monkhorst-Pack scheme[8] was used for the reciprocal space

sampling. The so-called TOLINTEG tolerance factors used for the Coulomb and exchange integrals were 8, 8, 8, 8 and 16. Default optimization convergence thresholds and integration grid for the exchange-correlation functional (XLGRID) were applied. In the harmonic frequency calculations, the SCF convergence threshold on total energy (TOLDEE) was set to 10^{-9} a.u.. IR intensities were obtained with the analytical coupled perturbed Kohn-Sham method.[10,11] The final IR absorbance spectrum is a superposition of Lorenzian peak shapes with FWHM of 16 cm^{-1}.

Additional basis set details

In periodic calculations, the Gaussian-type localized atomic basis set must be chosen carefully. Basis sets originally developed for molecular calculations contain diffuse basis functions to model the tails of wavefunction, but in periodic calculations, where the whole space is filled with basis functions, such diffuse functions are usually unnecessary and lead into numerical difficulties and/or severe degradation of performance.[12] The following triple-ζ-valence + polarization (TZVP) basis sets were applied here:

H, **C**, **O**: The basis sets were taken from a previous study.[13]

Li: The Karlsruhe def2-TZVP basis set was used as a starting point.[5] The most diffuse s- function was removed (exponent 0.029). The exponent of the most diffuse p-type function (0.06) was increased to 0.16 by dividing the second outermost p-exponent of 0.40 by a factor of 2.5. The exponent of the outermost s-type function (0.077) was then also increased to 0.16 by dividing the second outermost s-exponent of 0.51 by a factor of 3.2. Finally, the outermost s and p functions with an exponent of 0.16 were combined into a single sp-type function to increase the efficiency of the CRYSTAL code. The def2-TZVP basis set was thus changed from a (11s3p)/[5s3p] {62111/111} contraction pattern into (10s3p)/[4s3p] {6211/111}. The final basis set is listed below in CRYSTAL input format:

```
3 6
0 0 6 2.0 1.0
  6269.2628010      0.20540968826E-03
  940.31612431      0.15916554089E-02
  214.22107528      0.82869829707E-02
  60.759840184      0.33856374249E-01
  19.915152032      0.11103225876
  7.3171509797      0.27449383329
0 0 2 1.0 1.0
  2.9724674216      0.23792456411
  1.2639852314      0.30765411924
0 0 1 0.0 1.0
 0.51427489953      1.0000000000
0 1 1 0.0 1.0
```

```
 0.16                1.0 1.0
0 2 1 0.0 1.0
  3.327             1.0000000000
0 2 1 0.0 1.0
 0.40               1.0000000000
```

Table S1. The calculated structural parameters for Li_2Q

a	11.49 Å
b	10.38 Å
c	4.74 Å
Space group	*Pccn* (No. 56)

Atom	**Wyckoff position**	**x**	**y**	**z**	**Occ.**
O1	8e	0.66277	0.15466	0.23304	1.000
C1	8e	0.61710	-0.02804	0.52177	1.000
C2	8e	0.53541	0.89482	0.65708	1.000
C3	8e	0.58426	0.07961	0.35994	1.000
Li1	8e	0.67373	0.16467	0.83392	1.000
H1	8e	0.70884	-0.05241	0.53699	1.000
H2	8e	0.56397	0.81236	0.77993	1.000

Interpretation of the IR spectrum

All IR active modes from the vibrational calculations are collected in the table below. Modes were assigned by inspection of the normal modes visualized using the Jmol program.[14] Similar IR active modes are grouped together under one experimental peak.

Table S2. Interpretation of the experimental IR spectrum.

Corresponding experimental peak (cm^{-1})	Raw calculated frequencies (cm^{-1})	IR intensity (arb. units)	Irrep	Assignment
417	392	319	B_{1u}	Li breathing
	413	161	B_{2u}	
	422	653	B_{1u}	
453	435	7	B_{1u}	Li–O bend
	439	294	B_{3u}	
	448	1020	B_{3u}	

	458	504	B_{1u}	Li–O bend
	464	219	B_{2u}	
	489	1139	B_{2u}	
	495	301	B_{3u}	
	499	381	B_{1u}	
543	554	14	B_{1u}	Benzene ring out-of-plane bend
	563	1	B_{3u}	
	564	20	B_{2u}	
792	818	511	B_{3u}	C=C in-plane bending
	819	764	B_{2u}	
	831	428	B_{1u}	
839	855	356	B_{1u}	C–H out-of-plane symmetric bending
	856	186	B_{3u}	
	867	34	B_{2u}	
941	957	10	B_{1u}	C–H out-of-plane asymmetric bending
	968	20	B_{2u}	
	972	27	B_{3u}	
999	1018	3	B_{3u}	C–H symmetric bending
	1019	2	B_{1u}	
	1024	15	B_{2u}	
1094	1119	16	B_{3u}	C–H asymmetric bending
	1122	22	B_{2u}	
	1125	9	B_{1u}	
1245	1284	631	B_{3u}	C=C stretch
	1285	6	B_{2u}	
	1286	44	B_{1u}	
	1292	593	B_{3u}	
	1302	1510	B_{2u}	
1282	1334	218	B_{1u}	C=C stretch
1411	1458	93	B_{3u}	C=C stretch
	1462	19	B_{1u}	
	1463	49	B_{2u}	
1489	1536	1705	B_{2u}	C=O stretch
	1540	1254	B_{3u}	
1511	1572	616	B_{1u}	C=O stretch
3014	3173	81	B_{2u}	C–H stretch
	3178	5	B_{1u}	
	3179	9	B_{3u}	
3056	3191	23	B_{2u}	C–H stretch
	3194	1	B_{3u}	

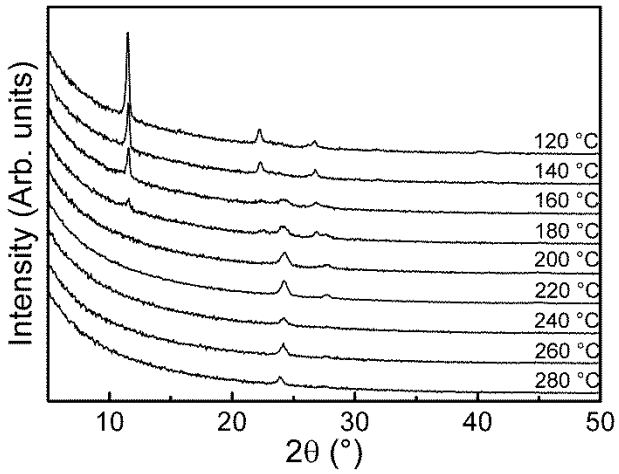

Figure S1. GIXRD patterns of Li_2Q samples deposited at different temperatures using 400 ALD/MLD cycles with pulse/purge lengths of 2.0s/2.0s and 10s/20s for LiHMDS and HQ, respectively.

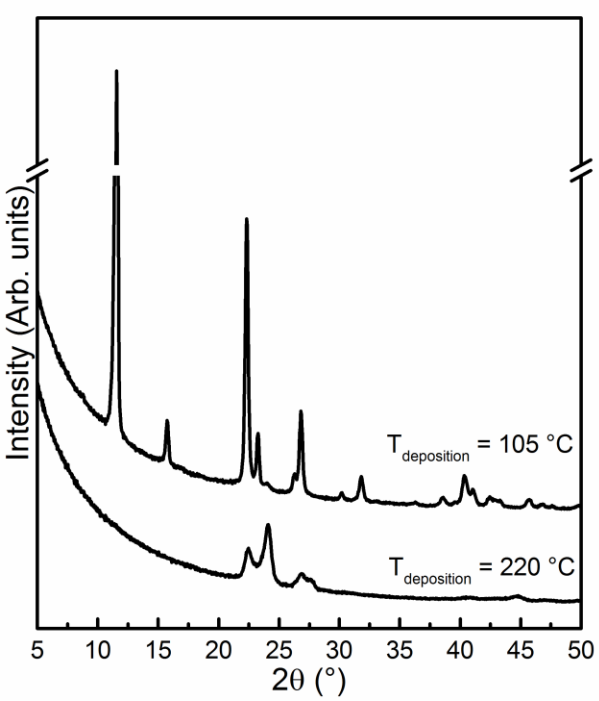

Figure S2. GIXRD patterns of Li_2Q samples deposited at 105 and 220 °C using 1600 ALD/MLD cycles with with pulse/purge lengths of 2.0s/2.0s and 10s/20s for LiHMDS and HQ, respectively. Full range of y-axis not shown for clarity.

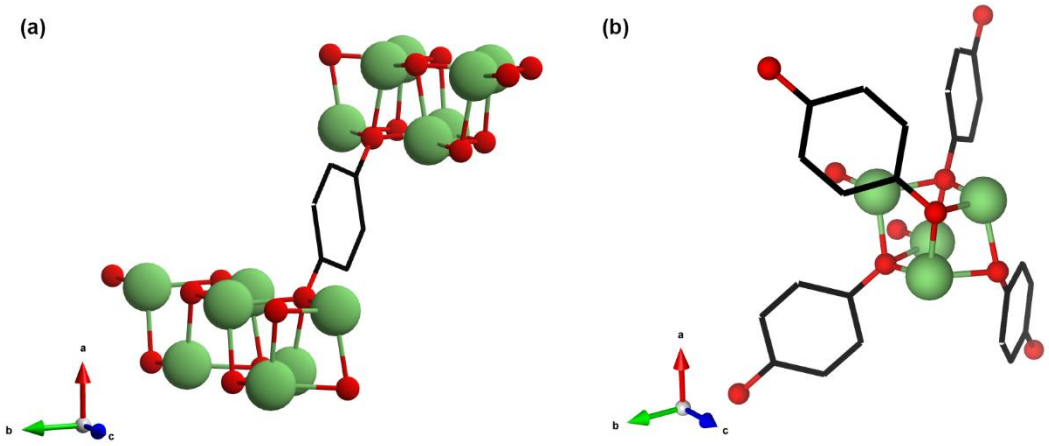

Figure S3. (a) The interconnectivity of the Li_2O_2 chains through a $[C_6H_4O_2]^{2-}$ unit (b) The secondary building unit resembling a lithium cubane cluster with the 3-coordinated lithium sites evident.

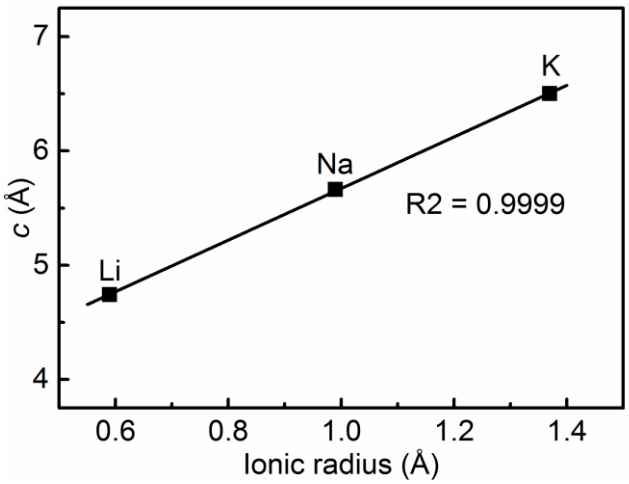

Figure S4. *c*-axis of the M_2Q compounds plotted against the ionic radii. Li: this work; Na, K from Couhorn and Dronkowski, *Z. Anorg. Allg. Chem*. 2003, ***629***, 647-652

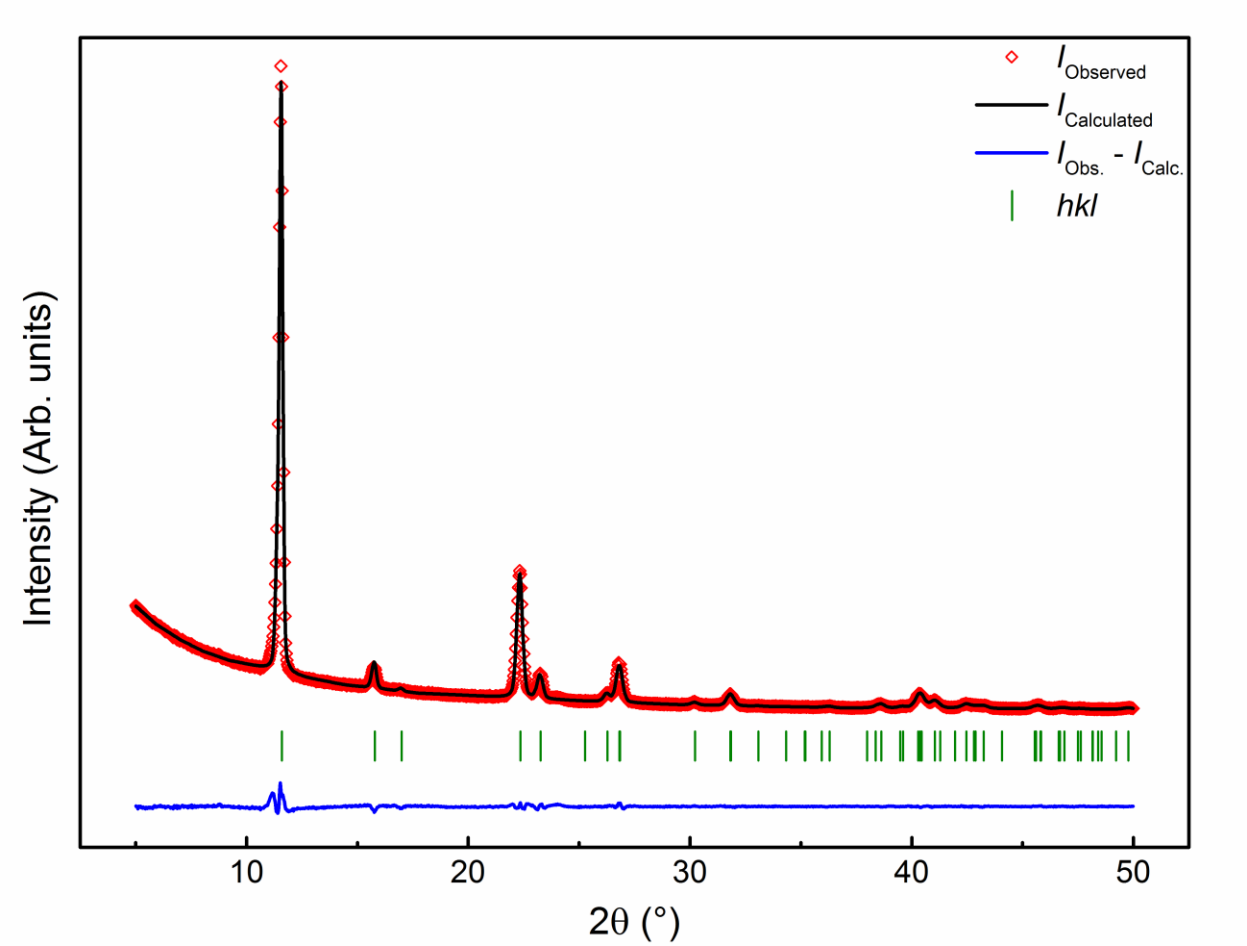

Figure S5. LeBail fit of the Li_2Q GIXRD pattern (deposition temperature: 105 °C) using the calculated orthorhombic *Pccn* space group. *a* = 11.25 Å, *b* = 10.45 Å, *c* = 4.66 Å. Rp = 11.6, Rwp = 9.44, χ^2 = 5.75

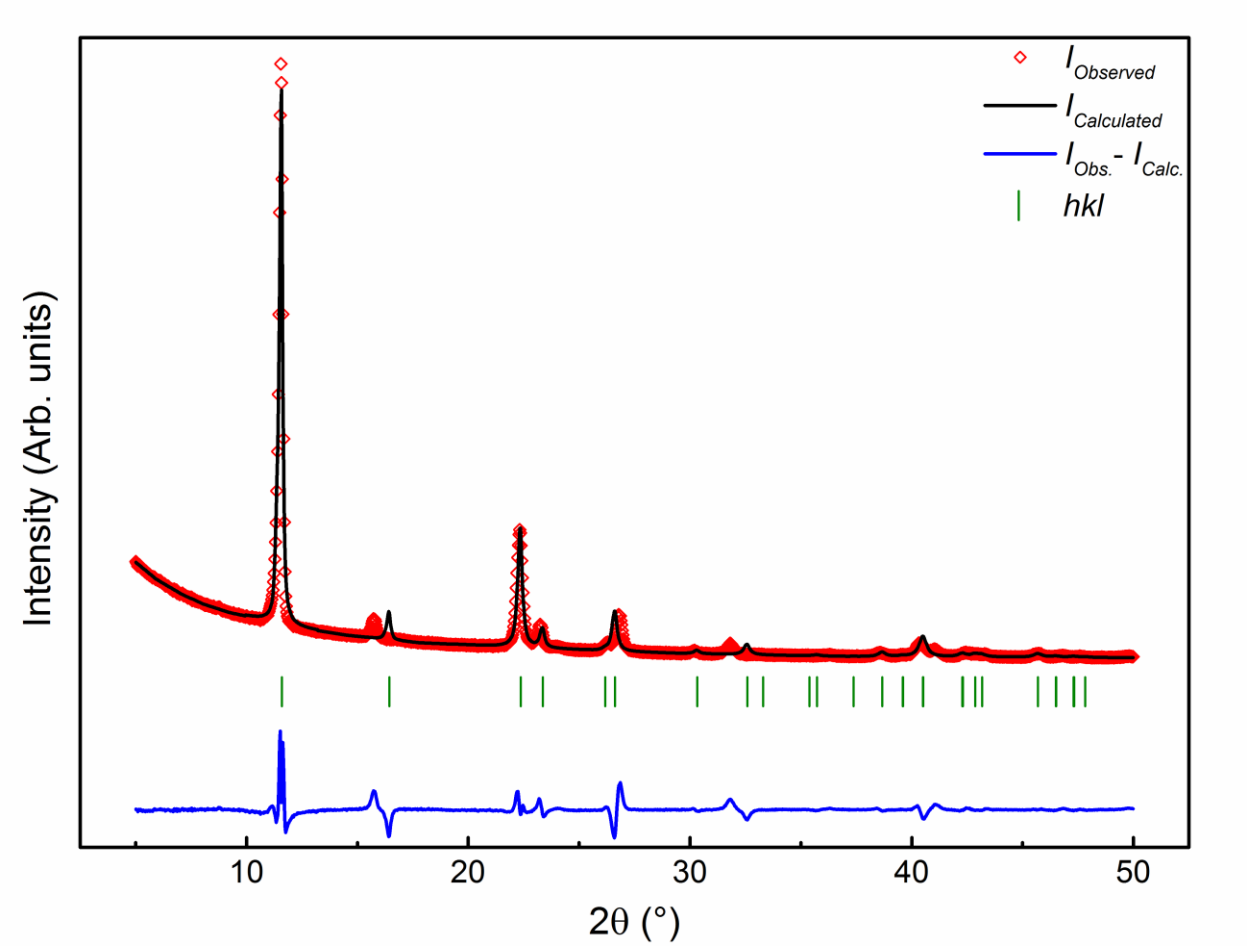

Figure S6. LeBail fit of the Li_2Q GIXRD pattern (deposition temperature: 105 °C) using the space group *P4₂/ncm* of Na_2Q shown here to demonstrate the inadequacy of the tetragonal symmetry to explain the observed GIXRD pattern. *a* = 10.74 Å, *c* = 4.65 Å. Rp = 35.3, Rwp = 41.3, χ^2 = 110

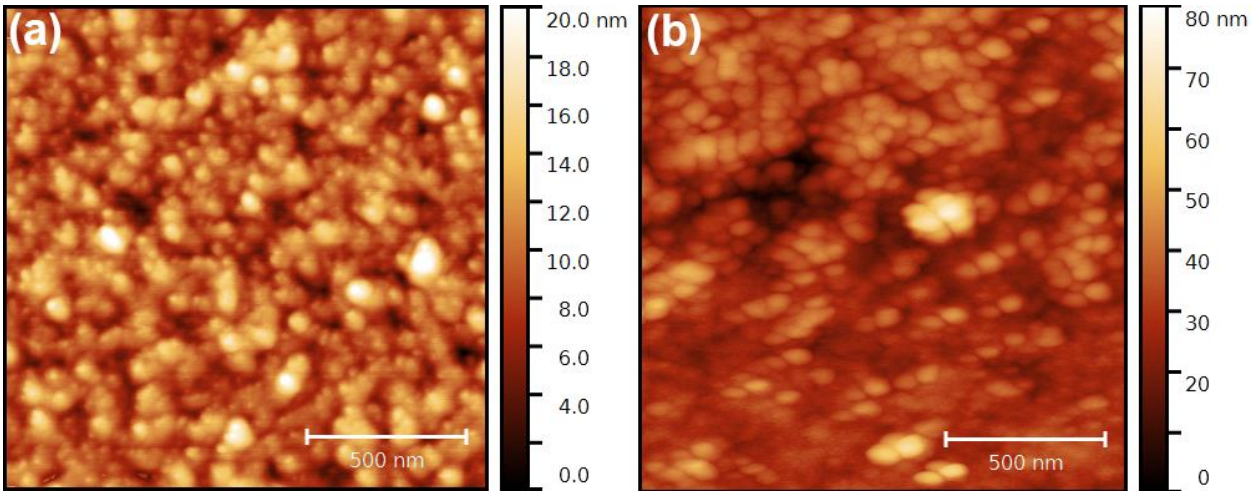

Figure S7. The AFM images obtained from (a) pristine, and (b) exposed samples. Note the differing depth scale.

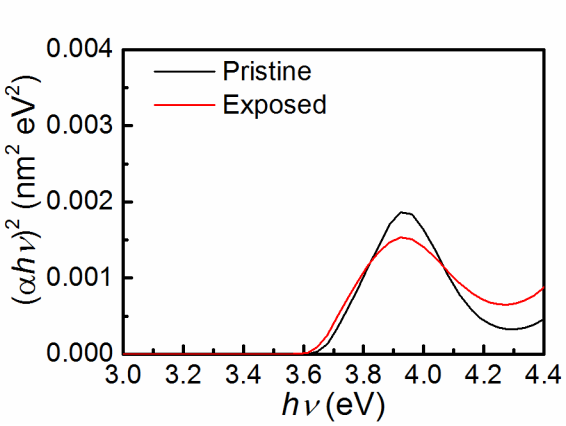

Figure S8. $(\alpha hv)^2$ vs hv plots for the pristine (black line) and exposed (red line) Li_2Q samples obtained from the UV-VIS measurements.

References for ESI material

1. Rodríguez-Carvajal, J. *Phys. B Condens. Matter* **1993**, *192*, 55–69

2. Dovesi, R.; Orlando, R.; Erba, A.; Zicovich-Wilson, C. M.; Civalleri, B.; Casassa, S.; Maschio, L.; Ferrabone, M.; De La Pierre, M.; D'Arco, P.; Noël, Y.; Causà, M.; Rérat, M.; Kirtman, B., CRYSTAL14: A Program for the Ab Initio Investigation of Crystalline Solids *Int. J. Quantum*

*Chem.***2014**, 114, 1287– 1317.

3**.** Dovesi, R.; Saunders, V. R.; Roetti, C.; Orlando, R.; Zicovich-Wilson, C. M.; Pascale, F.; Civalleri, B.; Doll, K.; Harrison, N. M.; Bush, I. J.;D'Arco, P.; Llunell, M.; Causà, M.; Noël, Y., *CRYSTAL14 User's Manual*; University of Torino: Torino, Italy, **2014**.

4. Pascale, F.; Zicovich-Wilson, C.M.; Gejo, F. Lopez; Civalleri, B.; Orlando, R.; Doveri, R., *J. Comput. Chem.*, **2004**, *25*, 888 -897.

5. Zicovich-Wilson, C. M.; Pascale, F.; Roetti, C.; Saunders, V.R.; Orlando, R.; Doveri, R., *J. Comput. Chem.*, **2004**, *25*, 1873-1881.

6. Perdew, J.P.; Burke, K.; Ernzerhof, M., *Phys. Rev. Lett.*, **1996**, *77*, 3865-3868.

7. Adamo, C.; Barone, V.; *J. Chem. Phys.*, **1999**, *110*, 6158-6170.

8. Weigend, F.; Ahlrichs, R., *Phys. Chem. Chem. Phys.* **2005**, 7, 3297–3305.

9. Monkhorst, H.J.; Pack, J.D., *Phys. Rev. B.*, **1976**, *13*, 5188-5192.

10. Maschio, L.; Kirtman, B.; Orlando, R.; Rèrat, M., *J. Chem. Phys.*, **2012**, *137*, 204113/1-204113/11

11. Maschio, L.; Kirtman, B.; Orlando, R.; Dovesi, R, *J. Chem. Phys.*, **2013**, *139*, 164101/1-164101/13.

12. Kudin, K.; Scuseria, G. E. *Phys. Rev. B* **2000,** *61***,** 16440–16453.

13. Karttunen, A.J.; Tynell, T.; Karppinen, M., *J.Phys.Chem. C.*, **2015**, *119(23)*, 13105-13114.

14. Jmol: an open-source Java viewer for chemical structures in 3D. http://www.jmol.org